

Chapter 7

Spatial Effects: Transport on Interdependent Networks

Richard G. Morris and Marc Barthelemy

Abstract Space plays an important role in the behaviour of both individual infrastructures, and the interdependencies between them. In this Chapter, we first review spatial effects, their relevance in the study of networks, and their characterization. The impact of spatial embedding in interdependent networks is then described in detail via the important example of efficient transport (or routing) with multiple sources and sinks. In this case, there is an optimal interdependence which relies on a subtle interplay between spatial structure and patterns of traffic flow. Although simplified, this type of model highlights emergent behaviour and brings new understanding to the study of coupled spatial infrastructures.

7.1 The Importance of Spatial Effects

Catastrophic failures in real world infrastructures are typically a result of consecutive improbable events. However, the chain of these events can often traverse more than one type of system, therefore it is important to understand the role of interdependency. For example, Fig. 7.1 shows a simplified schematic of interdependencies between various systems, and demonstrates how easily failures can propagate from one system to another.

Such interdependencies can be loosely classified into different categories [1]. For example, interdependencies can be ‘physical’, where the state of each system relies on the physical output of the other. In this case, one can imagine a coal-fired power station might generate the power for a rail network that, in turn, is used to deliver

R. G. Morris
The University of Warwick, Coventry, UK
e-mail: r.g.morris@warwick.ac.uk

M. Barthelemy (✉)
CEA-IPhT, Paris, France
e-mail: marc.barthelemy@cea.fr

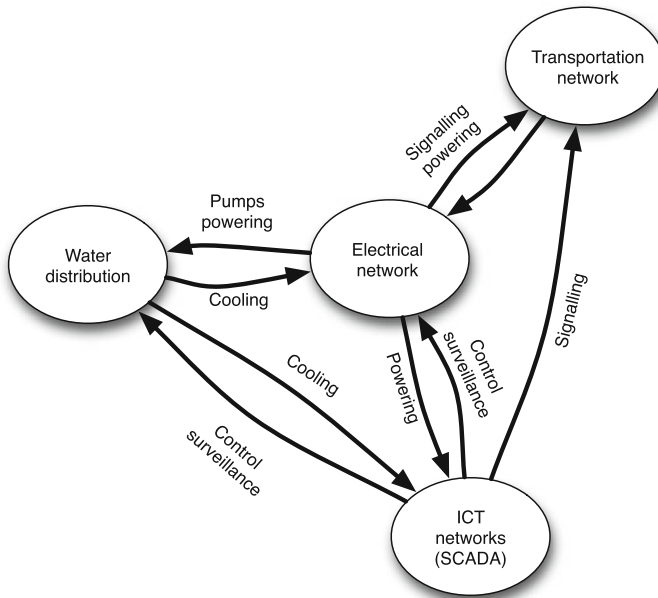


Fig. 7.1 Types of interdependencies between different critical infrastructures—adapted from Ref. [1]. Failure in the water distribution network might cause disruption at a power station, due to lack of cooling. This, in turn, could affect control networks employed to monitor water distribution in the first place, exacerbating the initial failure

coal to that same power station. We may also characterize ‘cyber’ dependencies, which is the case for example in supervisory control networks. Here, the state of one system relies on information about the state of the other system. The final type of interdependency can be described as ‘spatial’. That is, different systems can be affected by a localized disturbance due to spatial proximity. This simplest case relates to scenarios such as seismic failures, explosions, or fires, where an external event directly affects different infrastructures in the same location—and could be the trigger for a chain of failures. However, as we describe in later Sections, localized failure in one infrastructure may also be the cause of localized failure in another. For example, local traffic congestion on a road network can cause train overcrowding in the same region due to more people choosing the train.

This Chapter focusses on the last of these three classes, where transportation systems such as the road network, rail, subway, etc., are an important example. Such urban systems are, by construction, embedded in space and interdependent. However, an assessment of their resilience is very difficult [2], and therefore understanding the effect of interdependence on the stability of such systems is an important task [3]. One of the main problems is that human-mediated interdependency can be the source of counter-intuitive phenomena, such as flash congestion [4]. As a result, many detailed systems-engineering approaches have floundered, whilst the simplified models used

by physicists have proved helpful to identify the mechanisms underlying certain important characteristics. The aim of this Chapter is therefore to describe interesting effects that arise—at the aggregate level—for transportation systems that are both spatial and interdependent. To achieve this, the Chapter is organized as follows. In the next Section, spatial networks will be defined and their key properties reviewed. In Sect. 7.3, we describe, via two examples, how these properties affect systems of coupled networks. The final Section then concludes with a short recap and discussion of the main characteristics of such systems, whilst also highlighting open questions in the field.

7.2 Spatial Networks

Generally speaking, spatial networks are networks for which the nodes are located in a metric space—that is, one that permits the notion of a distance between any two points. Transportation and mobility networks, Internet, mobile phone networks, power grids, social and contact networks, neural networks, are all examples where space is relevant and where topology alone does not contain all the information [5]. For most practical applications though, it suffices to embed nodes in a straightforward two-dimensional euclidean space.

To give an idea of the role played by spatial effects, consider the following simple example. Imagine that a set of nodes are placed at random in the plane, and an edge is created between any pair of nodes according to some probabilistic rule. For spatial networks, this probability might decrease with the euclidean distance between the two nodes, for example. In this case, there is an implicit ‘cost’ associated with size of each edge, and therefore the connections between nodes are predominantly local. More broadly, the spatial constraints have had a dramatic effect on the resulting topological structure of the network.

Notice that the above definition does not imply that a spatial network is planar. Indeed, the airline passenger network, for example, is a network connecting direct flights through the airports in the world, and is not a planar network. Further to this, it is not even necessary that the embedded space of the network corresponds with a real space: social networks for example connect individuals through a friendship relations. The probability that two individuals are friends however generally decreases with the euclidean distance between them, showing that in social networks, there is an important spatial component (see for example [6]).

Whilst the above exceptions can be both important and interesting, in most systems of interest, both planarity and a real space embedding are natural choices. For example, electricity and gas distribution, roads, rail, and other transportation networks are all, to a very good approximation, spatial and planar networks. Due to the number of relevant examples and the intuitive ease with which they can be understood, we choose to focus primarily on such spatial-planar systems.

In the rest of this Section, therefore, we first review the main types of spatial networks and how they can be characterized. Then, with this in place, we describe

two important classes of problems that commonly feature spatial networks—failure cascade prevention and routing/transportation—and how they can be analyzed.

7.2.1 Types of Spatial Networks

There are, of course, many different types of spatial network. Indeed, as we describe in Sect. 7.2.2.1, choosing appropriate measures to classify different types of spatial networks is still an open area of research. However, for the purposes of this Chapter, it will suffice to look at only the broadest classes of spatial networks.

7.2.1.1 Regular Lattices

The simplest and most commonly used spatial network is the regular lattice—constructed by repeatedly copying a so-called ‘unit cell’. Whether a simple square lattice or one comprising more complicated polyhedra, the general properties are: uniform density, periodic structure and high degree of symmetry. In almost all cases, the unit cell is planar and very straightforward, where all nodes of the network have the same degree (although it is possible to use repeating units that are either non-planar or do not have uniform degree). Regular lattices are prevalent for two reasons, primarily due to their simplicity, but also due to the fact that many man-made systems have very regular structures such as the road network in many cities (e.g., Manhattan).

7.2.1.2 Delaunay Triangulations (and Voronoi Tessellations)

If the underlying system of study is planar, but a regular lattice has too much symmetry, one option is to use less regular types planar subdivisions. By far the most well-know of these are the Delaunay triangulation, and its dual, the Voronoi tessellation.

A Delaunay triangulation can be defined for any set of points positioned in the plane, the result being an almost¹ unique triangulation that maximises the smallest angle of all the triangles. That is, it tends to avoid very thin triangles. Given a particular Delaunay triangulation, one may construct the Voronoi diagram—a more general subdivision of the plane that associates a polygon with each node (see Fig. 7.2). There is a great deal of work that concerns the properties of such subdivisions and how to efficiently generate them, primarily due to their importance in problems of finding a so-called ‘convex hull’ for a discrete set of points. We refer the interested reader to the important work [7] which forms the cornerstone of most modern techniques for generating either Delaunay or Vornoi diagrams.

¹ If, in the exceptional circumstances that more than three nodes lie on the same circumcircle (see Fig. 7.2), then the neither the Delaunay or Vornoi diagrams are unique.

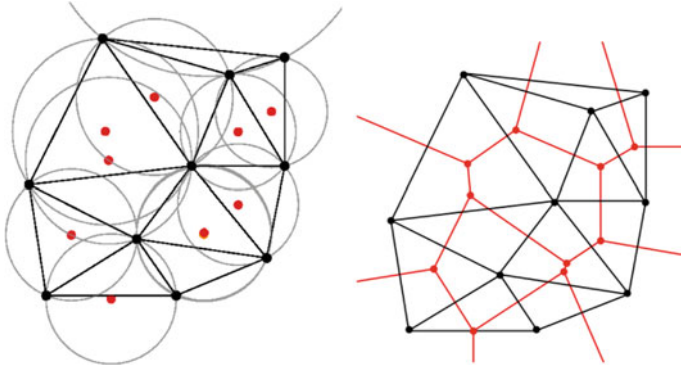


Fig. 7.2 A Delaunay triangulation is a triangulation of points (*black dots*) in the plane where the circumcircle of each triangle does not contain any other points. If the centres of circumcircles (*red dots*) belonging to neighbouring triangles are joined together, the Voronoi diagram is produced (*red lines*)

The benefit of such irregular planar subdivisions to the modeller is that one may specify a non-homogeneous distribution of nodes. For example, when representing a water distribution network, one might expect the result to be planar subdivision, but with greater density around towns and cities.

7.2.1.3 Probabilistic Networks

In order to incorporate more disorder, it is necessary to adopt a fully probabilistic approach to network generation. Here, one typically starts with a set of nodes positioned in the plane, and then, for each pair of nodes, creates an edge according to some probabilistic rule. The example discussed earlier considered a probability decreasing with the distance between two nodes, but this might equally involve more complicated spatio-topological indicators, such as clustering coefficients or average shortest paths (for more details on probabilistic models of spatial networks, we refer the interested reader to the review [5]).

7.2.2 Characterization of Spatial Networks

Whilst the first attempts to characterize spatial networks were made in the area of quantitative geography in the 1960s [8–11], more recently other measures have been popularized by the study of complex networks [12, 13]. Most of the currently used measures—often called indicators—are relatively simple, but still give important information about the spatial structure of the network. Here, we will briefly review the most useful quantities which allow for a good characterization of spatial networks.

7.2.2.1 Spatial and Topological Indicators

The most common quantities used to describe networks typically characterize only topological aspects and are not of particular interest for spatial networks. For example, the degree distribution is usually peaked which results from the fact that physical constraints imply a small cut-off, and the clustering and assortativity are usually flat, a consequence of the fact that connections are predominantly made to neighbors irrespective of their degrees.

A first useful quantity for spatial networks is the average shortest path ℓ which for most random networks scales as $\ell \sim \log N$ (where N is the number of nodes), signalling a small-world type behavior. In contrast, spatial networks are large-world and usually display a lattice-like behavior of the form

$$\ell \sim N^{1/d}, \quad (7.1)$$

where d is the dimension of the embedded space which, for most applications, is two.

Another helpful quantity used to characterize spatial systems, is the total length

$$L_{\text{tot}} = \sum_{e \in E} \ell(e), \quad (7.2)$$

where E is the set of edges and $\ell(e)$ is the Euclidean length of the edge e . Under the assumption of a peaked distribution of $\ell(e)$, the scaling for most networks is of the form

$$L_{\text{tot}} \sim L\sqrt{N}, \quad (7.3)$$

where L is the typical size of the area under consideration. One can then easily construct the minimum spanning tree on the same set of nodes and obtain its length $L_{\text{tot}}(MST)$. The ratio of these lengths

$$C = \frac{L_{\text{tot}}}{L_{\text{tot}}(MST)}, \quad (7.4)$$

is always larger than 1 and is a good measure of how costly a network is.

For some irregular planar subdivisions, like roads and railway lines, the polygons that make up the faces can correspond to important information about the structure of the network. We can characterize the faces by two main quantities, their area A and their shape factor

$$\phi = \frac{4A}{\pi D^2}, \quad (7.5)$$

where D is the largest diameter of the polygon. This quantity ϕ thus indicates how anisotropic the face is: for $\phi \approx 0$ the face is a very elongated rectangle and for $\phi \approx 1$

the face is essentially a disk. We observe for most road networks [5] the following behavior

$$P(A) \sim A^{-\gamma}, \quad (7.6)$$

where $\gamma \approx 2$, a value which probably finds its origin in the node density fluctuations [5].

The shape factor distribution usually displays a peak around $\phi \approx 0.6$ and its time evolution displays some interesting behavior which is so far unexplained [14].

We end this section by noting that the classic quantity, the betweenness centrality (BC) which quantifies the importance of a node (or an edge) in the network behaves very differently in spatial networks. In complex, scale-free networks, the BC scales as a power of the degree. In other words, the larger the degree the larger the BC, indicating that the hubs are the most important nodes in the network. In spatial networks, there is an interplay between the degree and the distance to the barycenter of nodes, leading to the appearance of ‘anomalies’, nodes with a small degree and a large BC.

7.3 The Effects of Interdependence in Spatial Networks

Studies that incorporate the features of coupled networks with those of spatial networks are small but growing in number. So far, such research has focussed on either failure cascades or transport and routing processes.

For failure cascades, the idea is that either the nodes or edges in the underlying system have an intrinsic carrying capacity which, if exceeded, causes a ‘failure’. Once an edge or node has failed, it is removed from the network and then redistributed. This may then cause the overloading and failure of further power lines, and so on. Such cascading failures are important because, under certain circumstances, small isolated failures can result in large system-wide outages. Recent work [15–21] has extended this idea to a system of interdependent networks—that is, the failure of a node in one network causes the immediate failure of the nodes to which it is connected in the second network. By measuring the size of the largest connected component that remains following a cascade, it can be shown that the extent of cascades increases as the number of inter-network connections is increased. In Refs. [23, 24], the authors apply this model of interdependent cascades to a system comprising two interdependent square lattice networks. Here, it is argued that since the model uses percolation techniques, the results—measured in terms of giant connected components—should not depend on the particular realization of the network. That is, it is known that the percolation transition has universal scaling behavior which does not depend on the coordination number and is the same for lattice and off-lattice models, as long as the links have a finite characteristic length [25]. The key aspect of the model is that dependency links between two networks are randomly chosen within a certain distance r . One can then show that percolation for small r is a second-order transition,

and for larger r is a first-order transition. Moreover, the results suggest that systems of this type become most vulnerable when the distance between interdependent nodes is in the intermediate range: greater than zero but much smaller than the size of the system.

As mentioned above, another class of systems that are both interdependent and spatial are general transport processes, or *flows* [22]. Whether flows of people, fluids, or electrical currents, these systems can be characterized by specifying the topology of the underlying network, a source-sink distribution, and a dynamic. To avoid confusion, we only imagine dynamical processes that converge to a steady state—resulting in a stationary distribution of flows over the network. Unfortunately, the methods of analysis mentioned above do not capture many of the typical features one might expect here. For example, it is easy to imagine a simple source-sink distribution that allows the network to be split into two distinct components such that the flows are unaffected. In this case, the size of the giant component may decrease but the network is still operating well.

Since the percolation techniques used to analyze cascading failures are well documented, the rest of this Chapter is devoted to the description of transport and routing processes.

7.3.1 *Transport and Routing*

One may ask: how should an interacting, or coupled, set of *flow* networks be characterized, and what are the interesting features of such systems? From observing real systems, one expects interesting effects to arise from three main areas:

- Spatial - and localization-effects from network connections.
- Spatial distribution of source and sinks.
- Coupling between the two networks.

Of course, the global behaviour of any real system is intimately linked with the particular form of dynamical interactions involved. However, some understanding of the above points can be gained by investigating the properties of simple examples that are chosen well enough to represent certain classes of systems. In this Section, we recap the results of examining such a ‘toy model’ [26], where the main idea is intuitively simple. Consider a transport network where there is a choice between travelling by train or by car, or perhaps the routing of packets in Information Communication Technology networks (ICT) where there are two different networks available (a simple schematic of this type of system is shown in Fig. 7.3). For these types of systems, the typical choice is between a ‘fast but sparse’ network and ‘slow but dense’ network. It is in this system that interesting effects arise through the interplay of the three main areas outlined above.

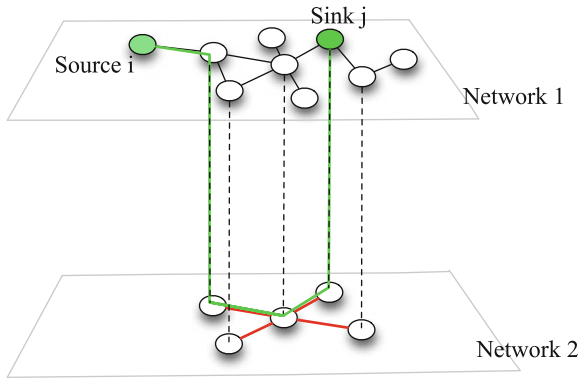


Fig. 7.3 Flows on two interdependent networks: edges of network 1 are shown in black, edges of network 2 are shown in red, and nodes in common to both networks are considered to be coupled (shown by *dashed lines*). Shown in *green*, we represent a path between two nodes, the ‘source’ i and the ‘sink’ j

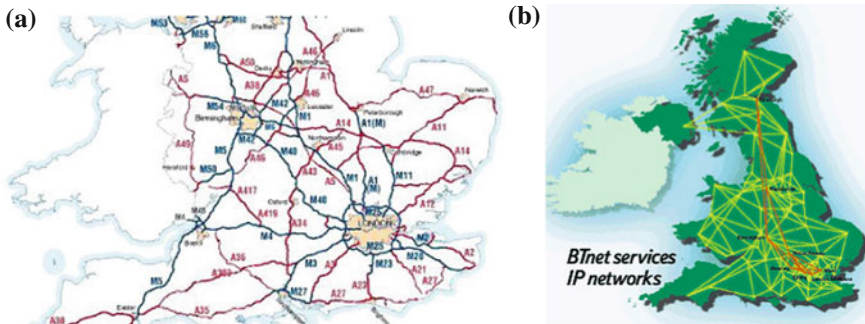


Fig. 7.4 **a** The national road network in England, and **b** the network of major internet servers across the UK operated by British Telecom. These networks are consistent with planar subdivisions on a finite sampling of nodes taken with uniform density

7.3.1.1 Network Structure

Since the motivation here is transport and routing problems, inspiration for the model can be found by looking at real systems. For example, one can argue that schematics of national transport networks or internet server networks resemble planar subdivisions where the nodes have been arranged at random with uniform density (see Fig. 7.4). Drawing from ideas discussed in Sect. 7.2.1, a good approximation for these systems is therefore to use Delaunay triangulations.

With the aforementioned examples in mind, one can ask: how should two Delaunay triangulations be coupled together? We imagine a road network coupled to a rail or subway network. Here, all the nodes of the road network are not nodes of the rail network, but conversely, all stations are located at points which can be considered

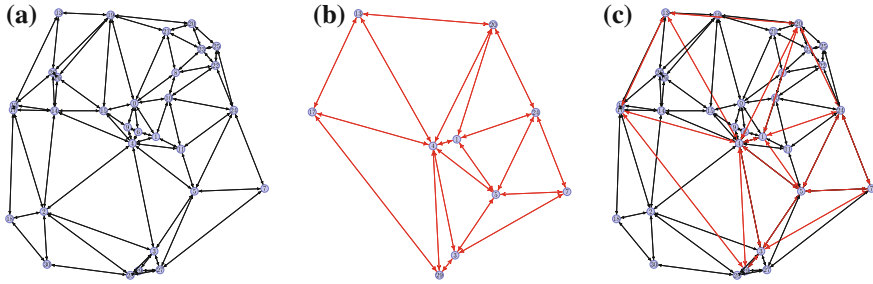


Fig. 7.5 Each instance of the system is generated according to the following process: **a** First, $N^{(1)}$ nodes (here $N^{(1)} = 30$) are positioned at random within the unit disk and the Delaunay triangulation is produced; **b** the second network is then generated by drawing $N^{(2)}$ (here $N^{(2)} = 10$) nodes uniformly from the existing ones ($N^{(2)} \leq N^{(1)}$) and, once again, computing the Delaunay triangulation; **c** the combined system is no longer planar

as nodes in the road network. That is, the nodes of one network are a subset of the nodes of the other. As will be shown, this setup conveniently provides a simple way to realize the ‘sparse’ versus ‘dense’ characterization described above.

More mathematically, one can construct two Delaunay triangulations $DT^{(1)}$ and $DT^{(2)}$. The set of nodes of $DT^{(1)}$ are taken to be $N^{(1)}$ points distributed uniformly at random within the unit disk. The nodes of $DT^{(2)}$ are then selected at random from $N^{(1)}$ and we define

$$\beta = \frac{N^{(2)}}{N^{(1)}} \leq 1. \quad (7.7)$$

That is, the model comprises two individual networks that are each planar Delaunay triangulations, forming a combined network that is not necessarily planar (see Fig. 7.5). For the combined network, $N = N^{(1)}$, and $E = E^{(1)} \cup E^{(2)}$. Recalling that Delaunay triangulations are effectively unique for a given set of points, it is then clear that, for a given value of β , the spatial and topological structure is entirely defined by $N^{(1)}$ and $N^{(2)}$.

7.3.1.2 Route Assignment

For modelling a transportation system, it is natural to associate a velocity $v^{(n)}$ with each network $n \in \{1, 2\}$, and to assign weights to each undirected edge $e^{(n)} = (\mathbf{x}_i, \mathbf{x}_j)$ according to

$$w(e^{(n)}) = \frac{|\mathbf{x}_i - \mathbf{x}_j|}{v^{(n)}}. \quad (7.8)$$

Here, w is the time taken to traverse the edge, and will provide the building block for all other useful system indicators.

To allocate flows on the network, rather than considering a dynamical system which acts to minimize a global quantity—such as electrical networks, where the dissipated power is minimized—a straightforward choice is to once again follow a transportation analogy. This means that the source-sink distribution of a general system of flows, can be replaced by an origin-destination (OD) matrix T_{ij} . Indeed, as before, this approach is also representative of the Internet, i.e., it is necessary to not only receive a packet of information, but it must be a particular packet sent from a particular server. Since each entry in the OD matrix specifies the proportion of the total flow that goes from node i to node j , this type of representation has the benefit that flows are completely specified by combining an OD matrix and a method of route choice.

The most obvious candidate for a method route choice, is to take the journey that minimizes the travel time. That is, the weighted shortest path, where the weights are given by Eq. (7.8). Here, the idea is that the ratio

$$\alpha = \frac{v^{(1)}}{v^{(2)}} \quad (7.9)$$

is a single parameter that controls the relative speed of travel on the two networks. Indeed, in order to simplify further, we impose the constraint that $\alpha \leq 1$. Since $\beta < 1$, this has the effect of enforcing the ‘fast but sparse’ versus ‘slow but dense’ scenario.

In terms of the OD matrix, it is impractical to consider the interplay between all possible forms for T_{ij} . Therefore it helps to choose a method that interpolates between two extremes, the monocentric case and a form of Erdős-Rényi random graph. We start with a monocentric OD matrix—i.e., all nodes travel to the origin—and then add noise by rewiring in the following way. For each node, with probability p , choose a random destination, and with probability $1 - p$, choose the origin (see Fig. 7.6).

7.3.1.3 Interdependence

Previous studies of interacting networks use the term *coupling* to describe how well two networks are linked. Typically, this is a purely topological definition i.e., the fraction of nodes from one network which link to another [15], or the probability that a particular node has an edge which connects both networks [20]. For transport processes, a better measure of interaction must include details of how the flows are distributed. For the system outlined above, we then specify a new quantity which we coin *interdependence* and is defined in a similar vein to the betweenness centrality

$$\lambda \equiv \sum_{i \neq j} T_{ij} \frac{\sigma_{ij}^{\text{coupled}}}{\sigma_{ij}}, \quad (7.10)$$

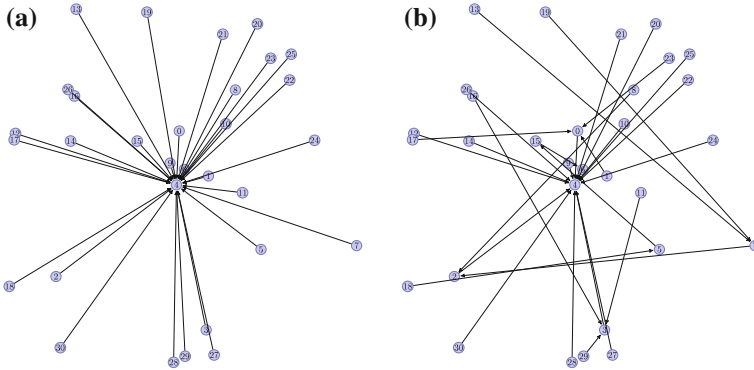


Fig. 7.6 Representations of OD matrices where each arrow corresponds to an entry in T_{ij} and which relates to the underlying geometry of Fig. 7.5. **a** A monocentric OD matrix. **b** A monocentric OD matrix randomly rewired with probability $p = 0.5$

where $\sigma_{ij}^{\text{coupled}}$ is the number of weighted shortest paths between nodes i and j , which include edges from *both* networks. In the transportation analogy, the interdependence is a way to quantify the importance of different transportation modes in order to achieve a fast journey. Here, the entries of the origin-destination matrix T_{ij} are normalized i.e., $\sum_{ij} T_{ij} = 1$, and it is clear from Eq. (7.10) that $\lambda \in [0, 1]$ is dependent on the method by which the flows are allocated and not just the system topology. The larger λ , the more one network is relying on the other to ensure efficient shortest paths (note that there is usually a maximum value of λ strictly less than one, since not all shortest paths can be multimodal). It is also clear that, by virtue of influencing the shortest paths, the number α can control the interdependence between the two networks.

With Eq. (7.10) in mind, instead of investigating the likelihood of catastrophic cascade failures, we consider more general measures of how well the system is operating. For example, one such measure is the average travel time

$$\tau = \sum_{i \neq j} T_{ij} w_{ij}, \quad (7.11)$$

where w_{ij} is defined from Eq. (7.8) as follows: $w_p = \sum_{e \in p} w(e)$ is the cumulative weight of path p , and $w_{ij} = \min_{p \in P} w_p$ is the minimum weight of all paths P between nodes i and j . For most practical transport processes, a well designed system reduces the average time travelled (i.e., water/food supply, the Internet, transportation, etc.).

Another important quantity, which can be used as a simple proxy for traffic flow, is the edge betweenness centrality (BC). For the system at hand, the definition of the edge BC is

$$b(e) = \sum_{i \neq j} T_{ij} \frac{\sigma_{ij}(e)}{\sigma_{ij}}, \quad (7.12)$$

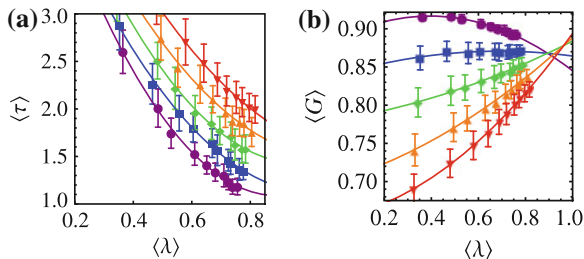


Fig. 7.7 Simulation results for the average shortest path and the Gini coefficient ($N^{(1)} = 100$, $N^{(2)} = 20$, and p values: 0 (purple), 0.2 (blue), 0.4 (green), 0.6 (orange), and 0.8 (red)). When the interdependence increases, the average shortest path decreases and the Gini coefficient can increase for large enough disorder (lines are polynomial fits)

where the sum is weighted by the proportion of trips T_{ij} , and $\sigma_{ij}(e)$ is the number of weighted shortest paths between nodes i and j , which use edge e . The betweenness centrality allows the introduction of a second measure, the Gini coefficient G . A number between zero and one, G is typically used in economics for the purpose of describing the concentration of wealth within a nation. Here it is used to characterize the disparity in the assignment of flows to the edges of a network, something that has been done before for transportation systems such as the air traffic network [27]. For example, if all flows were concentrated onto one edge, G would be one, whilst if the flows were spread evenly across all edges, G would be zero. We use the definition according to Ref. [28]

$$G \equiv \frac{1}{2|E|^2\bar{b}} \sum_{p,q \in E} |b(p) - b(q)|, \quad (7.13)$$

where subscripts p and q label edges, E is the total number of edges, and $\bar{b} = \sum_{p \in E} b(p)/|E|$ is the average ‘flow’ on the system. In this picture, the Gini coefficient can now be thought of as a measure of road use. A low value indicates that the system uses all roads to a similar extent, whilst a high value indicates that only a handful of roads carry all the traffic.

7.3.1.4 Existence of Optimal Interdependence

The set of numbers p , β and α , now define an ensemble of systems that are statistically equivalent (with respect to λ , τ , and G). Therefore one may calculate the quantities $\langle \lambda \rangle$, $\langle \tau \rangle$, and $\langle G \rangle$ for different values of p and α , where angle brackets $\langle \dots \rangle$ represent an ensemble average.

Simulation results are shown in Fig. 7.7, where each data point corresponds to an average over fifty instances of the OD matrix for each of fifty instances of the coupled network geometry. As the interdependence λ increases, the average journey

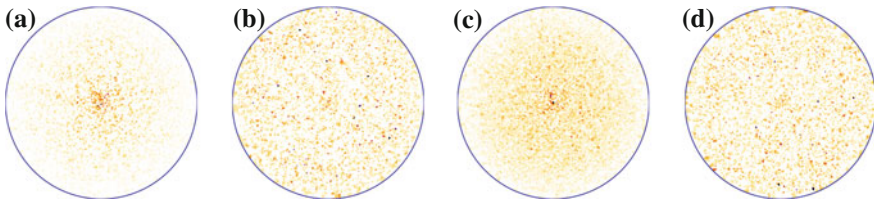


Fig. 7.8 Colormaps showing normalized edge flows—plotted at the midpoint of each edge—over many instances of the system. Colors are assigned starting from white (for zero flow) and moving through yellow, orange and red for higher values of flow, until reaching black (maximum flow). Each Subfigure corresponds to the following parameter values: **a** $p = 0.2$, $\alpha = 0.9$; **b** $p = 0.2$, $\alpha = 0.1$; **c** $p = 0.8$, $\alpha = 0.9$; **d** $p = 0.8$, $\alpha = 0.1$

time decreases (Fig. 7.7a). This is straightforward to understand since the increased interdependence is simply a result of reducing the velocity ratio α . Furthermore it is clear that increasing randomness in the origin destination matrix increases the length of the average shortest path by an almost constant value, irrespective of the interdependence. By contrast, the behaviour of the Gini coefficient at different interdependencies (Fig. 7.7b) is less easily explained. Consider instead Fig. 7.8. Here, each colormap shows the distribution of flows resulting from many instances of the system.

The first two plots, Figs. 7.8a and 7.8b, were generated from OD matrices rewired with low probability ($p = 0.2$) i.e., almost monocentric. The ratios of edge weights per unit distance between the two networks are $\alpha = 0.9$ and $\alpha = 0.1$ respectively. Therefore each diagram corresponds to a point on the blue line in Fig. 7.7b. For $\alpha = 0.9$, there is minimal independence between the networks and a high concentration of flows are seen around the origin. Since the flows are disproportionately clustered, this configuration is described by a high Gini coefficient. By contrast, for $\alpha = 0.1$, the difference in the edge weights means that it can be beneficial to first move away from the origin in order to switch to the ‘fast’ (low α) network. We therefore see a broader distribution of flows with small areas of high concentration around coupled nodes. The emergence of these *hotspots* away from the center also corresponds to a high Gini coefficient—and therefore the blue line in Fig. 7.7b is relatively flat. Figs. 7.8c and 7.8d correspond to the red line of Fig. 7.7b: generated from OD matrices rewired with high probability ($p = 0.8$). We observe that even for α close to one, the distribution of flows is broader than for $p = 0.2$ —resulting in a lower Gini coefficient. As α is decreased, the second network becomes more favourable and interdependence *hotspots* can be seen once again—resulting in a high Gini coefficient and a positive gradient for the red line of Fig. 7.7b. This result points to the general idea that randomness in the source-sink distribution leads to local congestion and more generally to a higher sensitivity to interdependence.

At this stage, it is natural to combine the effects observed above into a single measure. We assert that it is likely a designer or administrator of a real system would

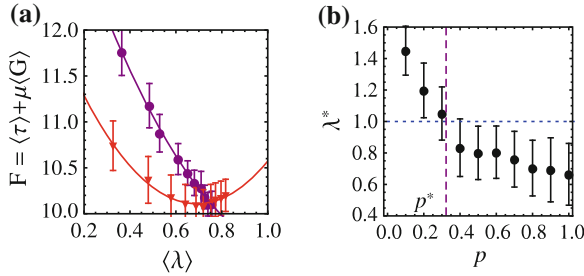


Fig. 7.9 Existence of an optimal interdependence: **a** Simulation results for $\mu = 10$, $N^{(1)} = 100$, $N^{(2)} = 20$, and p values: 0 (purple), 0.4 (green), and 0.8 (red) (three values only of p are shown to ensure the lines of best-fit can be seen clearly). **b** Minima of quadratic best-fit curves for different values of p . We obtain $\lambda = \lambda^*$ for $p^* \simeq 0.34$ (The error bars shown are those of the closest data point to the minimum of the best-fit curve)

wish to simultaneously reduce the average travel time and minimize the disparity in road utilization. To serve this purpose, a ‘utility’ function

$$F = \langle \tau \rangle + \mu \langle G \rangle \tag{7.14}$$

can be defined, where it is immediately apparent from Fig. 7.7 that, for certain values of μ , the function F will have a minimum. That is, a non-trivial (i.e., non-maximal) optimum λ will emerge. Figure 7.9a shows that, whether a non-trivial optimum interdependence exists depends on the origin-destination matrix. For OD matrices rewired with a high probability, increasing the speed of the rail network reduces the road utilization as flows become concentrated around nodes where it is possible to change modes. Dependent on the value of μ , the effect of reduced utilization can outweigh the increased journey time, leading to a minimum in F . Monocentric OD matrices, by contrast, have inherently inefficient road utilization when applied to planar triangulations, regardless of the speed of the rail network. Therefore no minimum is observed, and hence no (non-trivial) optimum λ . More systematically, one may plot the minima λ^* of best-fit curves corresponding to different values of p (Fig. 7.9b). Defining p^* , the value of p for which $\lambda^* = 1$, it is then possible to categorize the system into one of two regimes. We observe that: if $p < p^*$, then the optimal interdependence is trivially the maximum; otherwise if $p \geq p^*$, a non-trivial optimal interdependence exists.

7.4 Discussion and Perspectives

In this Chapter, we have highlighted the importance of spatial effects in coupled networks by focussing on problems of transportation and routing. In contrast to studies of failure mitigation—that often use either percolation or cascading-sandpile

techniques—models of transport are better described by measures of utility and efficiency. By using such quantities, it is possible to identify an optimal *interdependence* between the two networks. Below the optimum, the system is inefficient and travel times can be large, whilst above the optimum, system utilization is poor due to congestion arising around ‘link nodes’ that connect the two networks. The existence and behavior of this optimal value turns out to be very sensitive to the randomness of the individual trajectories that make up the system.

Even though the model is very simplified, it possesses the advantage of highlighting dominant mechanisms, and can serve as a basis for more sophisticated modeling such as the ones used and developed by civil engineers. The broader interpretation being that systems that rely on routing like transportation networks, or the Internet, may be inherently fragile to certain changes in supply and demand. Furthermore, if such observations can be generalized, this could have serious ramifications in other areas, such as the transition from centralized to de-centralized power generation [29].

Finally, we note that most studies have so far considered that the dynamical processes on the different interacting networks were the same. In many cases, this is not a realistic assumption, and it seems to us that an important future direction of research is understanding and classifying coupled systems where the dynamics are different. An example of this type of system are so-called *supervisory* control systems. Here, an underlying network such as the electrical distribution grid is coupled to an Information Communications Technology (ICT) network for the purposes of monitoring and control. For this case, failure spreading rules are different in each layer, and therefore the stability of the system is very difficult to predict [30].

Acknowledgments The authors thank financial support from CEA-DRT for the project STARC. MB was supported by the FET-Proactive project PLEXMATH (FP7-ICT-2011-8; grant number 317614) funded by the European Commission.

References

1. S. M. Rinaldi, J. P. Peerenboom, T. K. Kelly. Critical infrastructure interdependencies, *IEEE Control. Syst. Magn.* **21**,11 (2001).
2. D. Asprone, M. Cavallaro, V. Latora, G. Manfredi, V. Nicosia (2013).
3. R. H. Samet, *Futures* **47** 49–58 (2013).
4. C. Barrett, K. Channakeshava, F. Huang, J. Kim, A. Marathe, M. V. Marathe, G. Pei, S. Saha, B. S. P. Subbiah, A. K. S. Vullikanti, *PLoS One* **7**, e45406 (2012).
5. M. Barthelemy, *Phys. Rep.* **499**, 1 (2011).
6. D. Liben-Nowell, J. Novak, R. Kumar, P. Raghavan, A. Tomkins, *Proc. Natl. Acad. Sci. (USA)* **102**, 11623–11628 (2005).
7. L. Guibas and J. Stolfi, *ACM T. Graphic.* **4**, 74 (1985).
8. W. L. Garrison, *Regional Science* **6**, 121–137 (1960).
9. K. Kansky, *Structure of transportation networks: relationships between network geometry and regional characteristics* (University of Chicago Press, Chicago, 1969).
10. P. Haggett and R. J. Chorley, *Network analysis in geography* (Edward Arnold, London, 1969).
11. E. J. Taaffe and H. L. Gauthier Jr., *Geography of transportation*, (Prentice Hall, Englewood Cliffs, NJ, 1973).

12. J.-P. Rodrigue and C. Comtois and B. Slack, *The geography of transport systems*, (Routledge, New York, NY, 2006).
13. F. Xie and D. Levinson, *Geographical analysis*, **39**, 336–356 (2007).
14. E. Strano, V. Nicosia, V. Latora, S. Porta, M. Barthelemy, *Nature Scientific Reports* **2**:296 (2012).
15. R. Parshani, S. Buldyrev, and S. Havlin, *Phys. Rev. Lett.* **105**, (2010).
16. S. V. Buldyrev, R. Parshani, G. Paul, H. E. Stanley, and S. Havlin, *Nature (London)* **464**, 1025 (2010).
17. X. Huang, J. Gao, S. V. Buldyrev, S. Havlin, and H. E. Stanley, *Phys. Rev. E* **83**, 065101(R) (2011).
18. C.-G. Gu, S.-R. Zou, X.-L. Xu, Y.-Q. Qu, Y.-M. Jiang, D. R. He, H.-K. Liu, and T. Zhou, *Phys. Rev. E* **84**, 026101 (2011).
19. J. Gao, S. V. Buldyrev, H. E. Stanley, and S. Havlin, *Nature Phys.* **8**, 40 (2011).
20. C. D. Brummitt, R. M. D’Souza, and E. A. Leicht, *Proc. Natl. Acad. Sci. USA* **109**(12) (2012).
21. A. Saumell-Mendiola, M. A. Serrano, M. Boguna, arXiv:1202.4087, (2012).
22. S. Carmi, Z. Wu, S. Havlin, and H. E. Stanley, *Europhys. Lett.* **84**, 28005 (2008).
23. W. Li, A. Bashan, S. V. Buldyrev, H. E. Stanley, and S. Havlin, *Phys. Rev. Lett.* **108**, 228702 (2012).
24. A. Bashan, Y. Berezin, S. V. Buldyrev, and S. Havlin, arXiv:1206.2062, (2012).
25. A. Bunde and S. Havlin, *Fractals and Disordered Systems* (Springer, New York, 1991).
26. R. G. Morris and M. Barthelemy, *Phys. Rev. Lett.* **109**, 128703 (2012).
27. A. Reynolds-Feighan, *J. Air Transp. Manag.* **7**, 265 (2001).
28. P. M. Dixon, J. Weiner, T. Mitchell-Olds, and R. Woodley, *Ecology* **68**, 1548 (1987).
29. I. Lampropoulos, G. M. A. Vanalme, W. L. Kling, ISGT Europe 2010 IEEE PES (IEEE, New York, 2010).
30. R. G. Morris and M. Barthelemy. *Sci. Rep.* **3**, 2764 (2013).